COMPARISON OF REAL AND SIMULATED POLYCRYSTALLINE GRAIN STRUCTURES

PETR PONÍŽIL, IVAN SAXL, MILOSLAV DRUCKMÜLLER, JAROSLAV POKLUDA

The possibility to estimate grain size and grain dispersion by means of approximate relations based on properties of various 3D tessellation is examined on planar sections of simulated tessellations and of a real material. Estimates of the mean grain size volume based on the mean area of planar grain profiles and on the mean intercept length are compared and further improved by taking into account the profile area variance.

SROVNÁNÍ ZRN REÁLNÝCH A SIMULOVANÝCH POLYKRYSTALICKÝCH STRUKTUR

Na rovinných řezech simulovaných teselací a reálných materiálů byla ověřena možnost odhadu velikosti a rozložení zrn pomocí přibližných vztahů založených na vlastnostech různých 3D teselací. Byly srovnány odhady středního objemu zrn získané ze střední plochy řezů zrn a střední délky průsečíků zrn přímkou. Tyto odhady byly dále zpřesněny s použitím rozptylů ploch řezů zrn.

1. Introduction

From the geometrical point of view, grains can be considered as a space-filling division of the space into cells (grains) with disjoint interiors called a *spatial tessellation* [1–4]. Such a spatial tessellation induces a planar tessellation in any section plane and a line tessellation in any test line. The typical problem occurring in metallography is to infer the properties of a spatial tessellation from these induced tessellations. Perhaps the most important quantity is the intensity of grains λ (frequently denoted by N_V – the mean number of grains per unit volume). Clearly,

RNDr. P. Ponížil, Technical University Brno, Faculty of Technology, náměstí TGM 275, 762 72 Zlín, Czech Republic.

RNDr. I. Saxl, DrSc., Mathematical Institute, Academy of Sciences of the Czech Republic, Žitná 25, 115 67 Praha, Czech Republic.

Doc. RNDr. M. Druckmüller, CSc., Prof. RNDr. J. Pokluda, CSc., Faculty of Mechanical Engineering, Technical University Brno, Technická 2, 616 69 Brno, Czech Republic.

$\lambda = 1/\mathbf{E}v$, where $\mathbf{E}v$ is the mean grain volume. A vast literature exists on the subject, *e.g.* [3–11]. It is well known that the widely used linear intercept method estimates not the "grain size" however loosely defined but the mean surface area S_V of the grain boundaries per unit volume: $[S_V] = 2\lambda''$, where the intensity λ'' (frequently also N_L) is the mean number of intersected grains per unit length of the test line. Also the intensity λ' of grain sections (their mean number per unit area of the section plane) cannot be used to estimate λ because of the relation $\lambda' = \lambda \mathbf{E}b$, where the mean width (the mean Feret or caliper diameter) b is the mean length of projections of a grain into isotropic bundle of lines. An estimation of $\mathbf{E}b$ from planar section is possible only under strict assumptions concerning the grain shapes. Only then, the spatial grain size distribution can be estimated by so-called unfolding of profile size distribution. Unfortunately, the reliability of these methods [6, 7] imitating the procedures for estimation of isolated particle size distributions is rather poor as shown by simulation [12]. Isolated particles are primarily products of their growth processes which produce usually simple thermodynamically stable shapes. On the other hand, the primary goal of grains is to tessellate the space and simple shape assumptions are not justified. Unbiased grain sampling, which gives direct estimate of λ is possible only by means of 3D probes (disector, selector *etc.*). The application of these methods however difficult in opaque materials (a local comparison of two or several closely spaced parallel sections of known mutual distance is required – see [12, 13]) must be strongly recommended only if an *accurate* estimate of grain intensity λ is of primary importance.

Otherwise, less demanding approximate methods using particular properties of spatial tessellations can successfully meet less severe demands. They are based on a comparison of examined planar sections with 2D tessellations induced by various models of random spatial tessellations.

2. Models of random tessellations

A usual way of construction uses an idea of cell growth from germs generated by a random birth process. Let $\alpha(t)\mathrm{d}v\mathrm{d}t$ be the probability that a nucleus is born in the volume $\mathrm{d}v$ in the time interval $(t, t + \mathrm{d}t)$, where $\alpha(t)$ is the intensity of the point process in the four-dimensional half-space $\mathbb{R}^4_+ = \mathbb{R}^3 \times \mathbb{R}_+$. Whenever a germ is born its isotropic growth starts with a constant rate v under the condition that germs born within already growing cell are rejected and the growth is stopped in the points where two cells meet. Such a general tessellation is called the inhomogeneous *Johnson-Mehl tessellation* (JMT), the usual choice is $\alpha(t) = \alpha t^{-\beta}, \beta > -1$. Grain faces are pieces of hyperboloids of revolution, hence the cells are non-convex, nevertheless at least star-shaped with respect to the nucleus (any point of the cell is "visible" from its nucleus). Horálek [8] has shown that the ASTM grain size scale [14] can be satisfactorily approximated by the inhomogeneous JMT with $\beta = 1$. If $\alpha(t) = \alpha$, the birth process is a Poisson point process on the positive time axis and

the tessellation is (homogeneous) JMT. Finally, $\alpha(t) = \delta(0)$ (all nuclei are born at the time $t = 0$) gives the well known *Voronoi tessellation.* Its cells are convex polyhedra and any cell interior is the union of all points of the space lying closer to a germ ξ_i than to any other germ $\xi_j, j \neq i$.

Focusing the attention to the Voronoi tessellation, a collection of versatile models can be obtained by changing the pattern of germs. Orthorhombic point lattices produce uniform (all cells are translationally equivalent) orthorhombic tessellations covering a range of cell shapes from rectangular rods through cubes to plates. When the lattice points ξ_i are independently shifted by η_i following some centred 3-variate distribution (usually the coordinates of random shift vector have normal $N(0, \sigma^2)$ distribution), the resulting point pattern is called the *Bookstein model* on the given lattice (mostly cubic) and the tessellation generated by the pattern is the *Bookstein model tessellation* (BMT).

The *Poisson point process* (PPP) generates the *Poisson-Voronoi tessellation* (PVT). Its properties are well known either from theory or by means of large scale computer simulations [1, 15]. PVT plays the key role in the theory of random tessellations as well as in their statistics, namely, it is always used as a *null hypothesis* in statistical tests concerning tessellations [5, 11]. The Bookstein model on the cubic lattice with variance $\sigma^2 \to \infty$ tends to PPP and the corresponding BMT approaches PVT.

Clustered point patterns are commonly produced by implanting a point cluster Z into the points (called the *parents*) of PPP. Z is a finite bounded random set characterized by its cardinality N (the number of points forming Z), by its size (*e.g.* the diameter D of the ball into which any realization of Z can be included; $D = \sup(\operatorname{diam} Z)$), and by the arrangement of points (called the *daughters*). Instead of D, the dimensionless quantity $c = D/\rho_p$ is usually used, where ρ_p is the mean nearest neighbour distance of parents ($\rho_p = 0.554/\lambda^{1/3}$ for PPP of intensity λ in 3D space). In *Matérn clusters*, the daughters are arranged uniformly at random within the embedding ball and N has the Poisson distribution with the mean $\mathbf{E}N$. If $c \to \infty$, the cluster field with Matérn clusters approaches PPP of intensity $\lambda = \mathbf{E}N\lambda_p$.

The intensity λ of a tessellation is a scale parameter only, and, consequently, the knowledge of the properties of a unit tessellation ($\lambda = 1/\mathbf{E}v = 1$) is sufficient. The important characteristics of selected 3D unit tessellations (variance of cell volume $\operatorname{var} v$ and the average mean width $\mathbf{E}b$) and of the corresponding 2D sectional unit tessellations (variance of cell profile area $\operatorname{var} v'$) are given in Table 1 (the arrows indicate the above mentioned limit behaviour of BMT and CFT). A table including other properties is in [10].

It can be seen by inspection of Table 1 that there is some correlation between $\operatorname{var} v$ and $\operatorname{var} v'$ and that $\mathbf{E}b$ decreases with the increasing dispersion of cell volumes and profile areas (even when there is some difference between the values

Table 1. Selected characteristics of unit 3D tessellations (cubic (CUB)), Poisson-Voronoi (PVT), Matérn cluster field (CFT), Bookstein model on cubic lattice (BMT), homogeneous Johnson-Mehl (JMT), ASTM model (3D-ASTM), and of their planar sections (in the length units of $\lambda'^{-1/2}$!)

	M	CUB	BMT¶	PVT	CFT¶	JMT	3D-ASTM
3D	$\mathrm{var}\, v$	0	$\leftarrow \rightarrow$	0.1790	$\leftarrow$ 2.93	1.136§	2.047§
	$\mathbf{E}b$	1.5	$\leftarrow \rightarrow$	1.4580	$\leftarrow$ 1.112	1.238	1.146†
2D	$\mathrm{var}\, v'$	0.4?	0.4 $\rightarrow$	0.482	$\leftarrow$ 1.20	> 0.83	1.08§

† Calculated by Horálek [8] on assumption that ASTM is the inhomogeneous JMT with $\beta = 1$; $\beta = 0.9$ gives $\mathbf{E}b = 1.153$, the ASTM value is 1.155;
§ Calculated by Møller [16] for $\beta = 0$ and 1;
¶ Ponížil by simulation ($> 10^6$ cells for each choice of parameters); CFT for $c \geq 0.005$, $\mathbf{E}N \leq 30$, BMT for $0.005 \leq \sigma \leq 20$.

corresponding to convex and non-convex tessellations). This observation forms a basis of the following empirical approach.

3. Approximate estimation of $\mathbf{E}v$ and of $\mathrm{var}\, v$

In the paper [10], various methods of estimating properties of polycrystalline grain structure have been reviewed in detail. Here the attention will be focused on a rather moderate goal, namely

i. to estimate *approximately* the grain size as characterized by the mean grain volume $\mathbf{E}v$ or, equivalently, the grain intensity $\lambda = 1/\mathbf{E}v$ *i.e.* by the mean number of grains per unit volume,

ii. to characterize the spatial distribution of grains by comparing the observed 2D and 1D grain sections of a real polycrystalline material with tessellations induced in a plane and on a line by various models of random spatial tessellations – suitable quantities are the variances and coefficients of variations of grain volumes and of grain sections areas and lengths.

An approximate estimate $[\mathbf{E}v]$ is based on the generally valid equation [9, 10]

$$\mathbf{E}v = C' \, (\mathbf{E}v')^{3/2}, \quad C' = \left(\frac{\mathbf{E}b}{(\mathbf{E}v)^{1/3}} \right)^{3/2}, \tag{1}$$

where C' is a dimensionless global shape factor the values of which valid for various regular and random tessellations are presented and discussed in [10]. A tentative value $C' = 1.5$ is proposed there as a first approximation. Hence the relation

$$[\mathbf{E}v]_{v'} \approx 1.5[\mathbf{E}v']^{3/2}. \tag{2}$$

solves *i.* with an accuracy ±30%, say.

Another estimate based on the linear intercept method follows from an analog of Eq. (1)

$$[\mathbf{E}v]_{v''} = C''[\mathbf{E}v'']^3, \quad C'' = \left(\frac{\mathbf{E}s/4}{(\mathbf{E}v)^{2/3}}\right)^3, \tag{3}$$

where $\mathbf{E}v''$ is the mean chord length (or the reciprocal chord intensity λ'') and s is the surface area of grain (the assumption of grain convexity is important here). The value $C'' \approx 2.5$ is proposed in [10]. The accuracy is lower and the bounds of the numerical constant C'' are broader. It must be stressed that estimators (3) and to certain degree also (2) can give quite erroneous results if non-convex shapes and rugged boundaries make impossible a reliable decision which profiles compose the section of one grain.

The second aim is slightly more difficult. Cwajna *et al.* [9] proposed an empirical equation

$$[\mathrm{CV}(v)]_{\mathrm{CV}(v')} = K_1 + K_2 \ln[\mathrm{CV}(v')]. \tag{4}$$

Its advantage is that the coefficient of variation $\mathrm{CV}(v') = \sqrt{\mathrm{var}\, v'}/\mathbf{E}v'$ is a dimensionless quantity and can be simply estimated directly from images of planar sections (even without knowing the actual magnification etc.). A broader range of tessellations examined in [10] lead to slightly improved values $K_1 = 1.16$, $K_2 = 2.22$ (note that Eq. (4) seriously overestimates $\mathrm{CV}(v)$ for BMT with small values of σ; it gives $\mathrm{CV}(v) \approx 0.14$ instead of 0 at $\sigma \to 0$ – compare Fig. 1b in [10]). Combining now the both estimates (2) an (4) we obtain

$$[\mathrm{var}\, v]_{v'} = ([\mathbf{E}v]_{v'} \times [\mathrm{CV}(v)]_{\mathrm{CV}(v')})^2. \tag{5}$$

4. Examples

A) In order to prove the accuracy of the above-described approximate methods, several random tessellations have been simulated and examined together with their planar sections. The spatial intensity of generating points and, hence, also of the cells was $\lambda = 1/\mathbf{E}v = 1$ in all cases. Approximately 1000 cells in the sampled cube and 100 profiles per section remained for analysis after the spatial and sectional edge effects have been carefully removed, which is the number routinely encountered in metallographic analysis. Three types of spatial tessellations have been selected, namely PVT, two CFT's with clusters of Matérn type ($\mathbf{E}N = 5, 20$, $c = 0.005, 0.1, 1.0$) and finally, three BMT's with $\sigma = 0.005, 0.1, 1.0$. Examples of analysed planar sections are shown in Fig. 1, the numerical results of estimation are summarized in Tables 2 and 3. LSS are either the theoretical

Table 2. Estimates of $\mathbf{E}v$, $\mathrm{CV}(v)$, $\mathrm{var}\, v$, and λ'' in PVT and BMT

σ		$\mathbf{E}v$	$\mathrm{CV}(v)$	$\mathrm{var}\, v$	λ''	σ	$\mathbf{E}v$	$\mathrm{CV}(v)$	$\mathrm{var}\, v$	λ''
	LSS	1	0.423	0.179	1.455		1	0.006	0.00004	1.494
PVT	Real.	0.983	0.412	0.170		0.005	0.993	0.006	0.00004	
	Est.	0.836	0.319	0.081			0.834	0.077	0.128	
	CE	0.099	0.148	0.054			0.135	0.415	0.248	
	LSS	1	0.101	0.010	1.432		1	0.402	0.1618	1.458
0.1	Real.	0.998	0.102	0.010		1.0	1.02	0.411	0.169	
	Est.	0.951	$-$ (<0)	–			0.837	0.241	0.057	
	CE	0.143	–	–			0.096	0.187	0.060	

Table 3. Estimates of $\mathbf{E}v$, $\mathrm{CV}(v)$, $\mathrm{var}\, v$, and λ'' in CFT's

c		$\mathbf{E}N$	$\mathbf{E}v$	$\mathrm{CV}(v)$	$\mathrm{var}\, v$	λ''	$\mathbf{E}N$	$\mathbf{E}v$	$\mathrm{CV}(v)$	$\mathrm{var}\, v$	λ''
	LSS		1	0.994	0.988	1.484		1	1.48	2.19	1.309
0.005	Real.	5	0.997	0.834	0.7		20	0.98	1.43	2.06	
	Est.		0.789	0.94	0.563			1.16	1.39	2.68	
	CE		0.181	0.138	0.273			0.3	0.10	1.19	
	LSS		1	0.975	0.952	1.479		1	1.47	2.15	1.317
0.1	Real.	5	1.02	0.84	0.709		20	1.06	1.51	2.29	
	Est.		0.802	0.98	0.64			1.30	1.30	2.98	
	CE		0.108	0.131	0.224			0.34	0.19	1.56	
	LSS		1	0.857	0.735	1.456		1	1.27	1.61	1.369
1.0	Real.	5	1.05	0.808	0.656		20	0.97	1.19	1.43	
	Est.		0.858	0.831	0.545			0.93	1.35	1.59	
	CE		0.133	0.080	0.255			0.13	0.12	0.44	

values (PVT) or the values obtained by large scale simulations; in these rows also the intensity λ'' is given. Note that it changes whereas the mean grain volume is constant! Real. are the sample means from 10 cubes each of which contained approximately 1000 cells. Est. are the mean values of estimates from 10 planar sections (one per each cube) and CE are the coefficients of error of these means (the standard deviation of the sample mean divided by sample mean).

B) Planar sections of commercial construction steel ČSN 11 301.0 (0.1% C, 0.4% Mn) specimens have been polished and etched in 1% Nital solution to reveal the grain structure (Fig. 2). The profile areas (two sections, 1850 profiles) have been estimated by means of an automatic image analyser under final magnification 246× and then a numerical correction on the non-zero thickness of grain boundary traces was applied. Moreover, the intensity $\lambda'' = 1/\mathbf{E}v''$ was estimated by manual

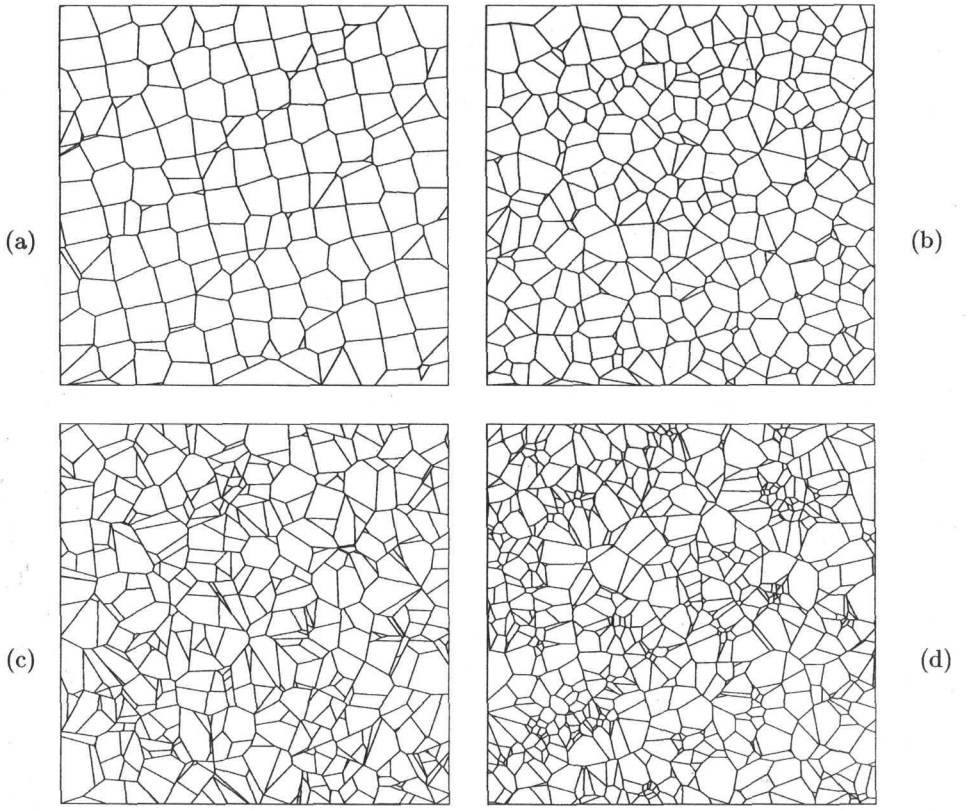

Fig. 1. Examples of examined planar sections: (a) BMT ($\sigma = 0.1$), (b) PVT, (c) CFT ($c = 0.005$, $\mathbf{E}N = 5$), (d) CFT ($c = 1.0$, $\mathbf{E}N = 20$).

analysis. The results are as follows: $[\mathbf{E}v'] = 1115\,\mu\text{m}^2$, $[\mathbf{E}v''] = 31.81\,\mu\text{m}$, $\text{CV}(v') = 0.919$. Then from Eq. (2) is $[\mathbf{E}v]_{v'} = 55850\,\mu\text{m}^3$, whereas Eq. (3) gives $[\mathbf{E}v]_{v''} = 80480\,\mu\text{m}^3$. Finally, $[\text{CV}(v)]_{\text{CV}(v')} = 0.972$ by Eq. (3) and a comparison with Tables 1–3 leads to the conclusion that the analysed grain structure reveals a distinct features of a cluster field tessellation.

5. Discussion

ad A) The chosen models cover a rather broad class of situations. BMT's with $\sigma = 0.005$ and 0.1 are tessellations induced by quasi-uniform hard-core point patterns, which are close to the cubic tessellation. The uniformity of cells and of

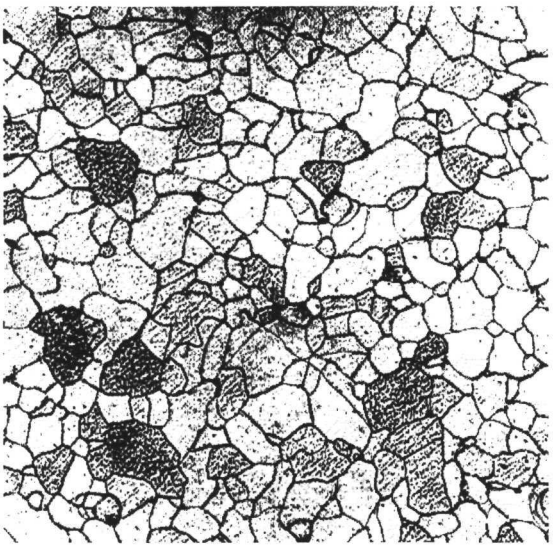

Fig. 2. A part of examined planar sections of the real material (magnification 132×).

their arrangement is already lost at $\sigma = 1.0$ and $\operatorname{var} v$ approaches the PVT value.

The two cluster fields differ considerably. At $\mathbf{E}N = 5$ and small c, the parent cells are divided more or less regularly into pyramid-like *outer* cells generated by the daughters having at least one nearest neighbour belonging to another cluster. At $\mathbf{E}N = 20$, many so-called *inner* cells also occur; they are associated with daughters completely encircled by points of the same cluster. Inner cells are much smaller than the outer ones and, thus, the whole cell populations is a mixture of cells of two kinds differing in size and shape. With growing c this difference slowly vanishes.

a) *Estimates of* $\mathbf{E}v$: The more accurate value of C' for PVT, BMT a CFT with $\mathbf{E}N = 5$ lies between 1.7 and 1.8 (see [10]), hence a negative bias of the estimate is observed. Similarly for CFT with $\mathbf{E}N = 20$ is C' as low as 1.2, hence a positive bias of the same order is observed. Even when CE is rather high for small clusters with high $\mathbf{E}N$ (the samples are too small for a population with such a high dispersion of sizes), the accuracy of the estimator $[\mathbf{E}v]$ lies within the expected range ±30%.

b) *Estimates of* $\mathrm{CV}(v)$ *and of* $\operatorname{var} v$: A negative bias typically below 0.1 prevails in CFT's. Taking into account small sizes of the planar samples, this result is surprisingly good. A high positive bias in BMT's with $\sigma = 0.005$ and a negative value at $\sigma = 0.1$ demonstrate limited validity and instability of estimates based on Eq. (3) in such cases. Slightly surprising is the high negative bias of $\mathrm{CV}(v)$ in the case of PVT. Nevertheless, the order of increasing $\mathrm{CV}(v)$ from BMT to PVT,

CFT with $\mathbf{E}N = 5$ up to CFT with $\mathbf{E}N = 20$ is correctly reflected by the obtained estimates.

The biases in the both previous estimates combine and the result is moreover squared in $[\mathrm{var}\, v]_{v'}$; nevertheless, at least the estimates in CFT's are still acceptable.

ad B) In the examined real material, the difference between the mean grain volume estimates $[\mathbf{E}v]_{v'}$, $[\mathbf{E}v]_{v''}$ can be diminished by the application of more accurate values of C', C''. Namely, the value of $\mathrm{CV}(v)$ reveals that the dispersion of grain sizes is comparable with the examined CFT ($N = 5$) for which $C' \approx 1.75$ (see above A.a)). From a similar reason (see [10]), the value of $C'' \approx 2.3$ is perhaps more appropriate. The improved estimates are $[\mathbf{E}v]_{v'} = 65158\,\mu\mathrm{m}^3$ and $[\mathbf{E}v]_{v''} = 74041\,\mu\mathrm{m}^3$. $[\mathbf{E}v]_{v'}$ is in any case more reliable. First, a planar section is a more representative image of 3D structure than a line section and, moreover, in view of rather thick boundaries, some small secants can remain unobserved in the neighbourhood of three profile junctions. Inserting for C' in Eq. (1), an estimate of $[\mathbf{E}b]_{v'} = [\lambda']_{v'}/[\lambda]^{2/3} = 1.45$ (in the length units of $\lambda^{-1/3}$, hence comparable with the values in Table 1) for the real material (only slightly lower than the PVT value) is an acceptable value for a tessellation with mild clustering ($N = 5$, say), whereas from $[\lambda]_{v''}$ an unreasonably high value of $[\mathbf{E}b]_{v''} = 1.58$ follows.

6. Conclusions

The analysis of small size samples of simulated tessellations confirmed a good reliability of the proposed mean grain volume estimates. The proposed common value of $C' = 1.5$ ensured the accuracy within the expected $\pm 30\%$ layer even in considerably different cases covering a range of situation from nearly uniform to highly non-uniform cell populations. The observed bias of the estimate can be further decreased by a selective choice of C' according to the estimated value of the coefficient of variance of profile areas. Moreover, the estimated value of $\mathrm{CV}(v)$ correctly reflects the tendency to clustering or to uniformity in the examined tessellations.

The examination of a real tessellation has shown an appreciable difference between the mean grain volume estimates based on the mean profile area and on the mean intercept length. The estimate of $\mathrm{CV}(v)$ made possible a selective choice of factors C', C'', which narrowed the difference between these estimates considerably. The mutual comparison of estimates of $\mathbf{E}b$ then confirmed the estimate based on the mean profile area as a more reliable. Thus, the usefulness of the variance estimation has been proved in the both analysed cases. In fact, the approximate estimation based on the use of Eqs. (2) and (3) with fixed values of C, C'' would be no substantial improvement in comparison with the conventional characterization of grain size by the values of λ', λ'' (N_A, N_L in another notation) only.

It must be stressed that simulations of tessellations serving as models of real polycrystalline grain structures become very important also with respect to spe-

cial fracture analyses like intergranular crack growth modelling and assessment of associated shielding effects at the crack front [17].

Acknowledgements. This research was supported by the Grant Agency of the Czech Republic (contract No. 201/1996/0226 – I.S.) and by the grant of the Ministry of Education of the Czech Republic (contract No. 96108 – P.P.).

REFERENCES

[1] OKABE, A.—BOOTS, B.—SUGIHARA, K.: Spatial Tessellations. Chichester, Wiley 1992.
[2] MØLLER, J.: Lectures on Random Voronoi Tessellations. Lecture Notes in Statistics 87. New York, Springer-Verlag 1994.
[3] STOYAN, D.—KENDALL, W. S.—MECKE, J.: Stochastic Geometry and its Applications. New York, Wiley 1995.
[4] SAXL, I.—PELIKÁN, K.—RATAJ, J.—BESTERCI, M.: Quantification and Modelling of Heterogeneous Systems. Cambridge, Cambridge Int. Science Publishing 1995.
[5] LORZ, U.: Materials Characterization, *25*, 1990, p. 297.
[6] SCHÜCKHER, F.: In: Quantitative Microscopy. Eds.: DeHoff, R. T., Rhines, F. N. New York, McGraw-Hill Book Comp. 1968, p. 201.
[7] UNDERWOOD, E. E.: Quantitative Stereology. Reading, Adison Wesley Publ. Comp. 1970.
[8] HORÁLEK, V.: Materials Characterization, *25*, 1990, p. 263.
[9] CWAJNA, J.—CHRAPOŃSKI, J.—MALIŃSKI, M.: In: Proc. of Int. Conf. on the Quantitative Description of Materials Microstructure. Eds.: Wojnar, L., Rożniatowski, K., Kurzydłowski, K. J. Jagiellonian University Kraków, 1997, p. 27.
[10] SAXL, I.—PONÍŽIL, P.: In: Proc. of Int. Conf. Fractography 97. Ed.: Parilák, Ľ. Košice, Inst. Mat. Res., Slovak Acad. Sci. 1997, p. 132.
[11] HAHN, U.—LORZ, U.: J. Microsc., *175*, 1994, p. 176.
[12] CHRAPOŃSKI, J.– MALIŃSKI, M.: In: Proc. of Int. Conf. on The Quantitative Description of Materials Microstructure. Eds.: Wojnar, L., Rożniatowski, K., Kurzydłowski, K. J. Jagiellonian University Kraków, 1997, pp. 215, 223, 229.
[13] KARLSSON, L.M.—CRUZ-ORIVE, L. M.: J. Microsc., *165*, 1992, p. 391.
[14] ASTM E 112-82: Standard Methods for Determining Average Grain Size (1982).
[15] LORZ, U.—HAHN, U.: Geometric Characteristics of Random Spatial Voronoi Tessellations and Planar Sections. Preprint 93-05. Freiberg, Bergakademie Freiberg 1993.
[16] MØLLER, J.: Adv. Appl. Prob., *27*, 1995, p. 367.
[17] HORNÍKOVÁ, J.—ŠANDERA, P.: In: Proc. of Int. Conf. Fractography 97. Ed.: Parilák, Ľ. Košice, Inst. Mat. Res., Slovak Acad. Sci. 1997, p. 169.

Received: 17.6.1998